Proceedings of the
International Conference on Mechanical Engineering and Renewable Energy 2017
(ICMERE2017) 18 – 20 December, 2017, Chittagong, Bangladesh

ICMERE2017-PI-254

SIZE DEPENDENT STUDY OF MECHANICAL PROPERTIES OF COBALT THIN FILMS UNDER UNIAXIAL AND BIAXIAL TENSION

Shahriar Nahian[1], Arefin Mustafa Anik[2], Tawfiqur Rakib[3], Satyajit Mojumder [4]

[1-4]Department of Mechanical Engineering, Bangladesh University of Engineering and Technology
Dhaka-1000, Bangladesh
shahriarnahian2015@gmail.com*, arefinmustafaanik@gmail.com, tawfiq1448@gmail.com,
satyajit@me.buet.ac.bd

Abstract- *The mechanical properties of Cobalt thin film have been an important issue due to its application as magnetic films in electronics and biomedical field. Being subjected to numerous applications, its mechanical properties remain a key issue. In this paper, molecular dynamics simulations are conducted to find the mechanical properties of Cobalt (Co) thin film. Embedded Atom Method (EAM) potential is employed to define the atomic interactions between Co atoms.The present study shows the mechanical properties and failure mechanism of Cobalt thin films under uniaxial and biaxial tension as its thickness (t) varies in the range of t=2~10nm.The result shows that the ultimate tensile strength decreases with the increase of thickness of the thin films. Finally, failure mechanisms are shown in consecutive atomic images.*

Keywords: Molecular Dynamics, Tensile Strength, Stress Concentration, Thin Film, Atomic Potential

1. INTRODUCTION

In the past few years, researchers have grown an interest in nano science and technology. Using structure at micron and nano level is the key to the development of electronic devices and elements of micro/nano electromechanical system (MEMS/NEMS). For scientific and engineering purposes it is important to study and understand the mechanical properties. In recent years, great interest has been shown on nanowires and other one-dimensional systems due to their potential in different types of applications. Different types of nanowires have been developed using chemical routes such as laser assisted catalytic growth. The mechanical strength of nanowires is necessary to maintain the structural integrity of the systems.

Over the last past few years' computer simulation technique was developed to determine the mechanical properties. Simulations using molecular dynamics method are capable of unveiling some processes to explain the fundamental mechanism of dislocation formation, plastic region and breaking of nanomaterial under stress.

Recently many researchers have studied the tensile deformation of nanowires under uniaxial tension using numerical methods such as molecular dynamics. Komandari et al. [1,2] used Morse potential for modeling BCC and FCC nanowires. They found that the two body potentials could not predict the tensile behavior of BCC metals accurately. Park et al. [3, 4] simulated the tensile test for FCC nanowires with different crystallographic orientations. Recently Wu [5, 6] studied the mechanical properties of the copper nanowire at different temperatures, sizes and strain rates. Golovnev [7] developed more results on copper nanowires. Lin Yuan et al. [8] studied aluminum nanocrystal under the uniaxial tension at different temperatures. Branico and Rino [9] investigated the failure mechanism of Ni nanowires. Wena et al. [10] employed the molecular dynamics simulation with quantum corrected suttenchen type many body potential for Ni nanowire at room temperature.

Further studies on the mechanical behavior of nanowires with various loading, Parinello and Rahman [11] introduced a new Lagrangian formulation to perform MD simulations on systems under external stress. Using this method, they applied uniaxial stress to an FCC cubic lattice (Ni) with periodic boundary conditions at $350\ K$. Under uniaxial compression, they suggested a transformation in the crystal structure from FCC to HCP. The maximum tensile strength under uniaxial tension was reported to be 11 × 1010 dyn/cm^2. Kitamura et al[12] conducted atomic simulations of tension on a nanoscopic wire, film, and bulk of a Ni lattice without defects. To investigate the effect of constraint of transverse deformation on the fracture process, simulations for the bulk were conducted under two conditions: free transverse stress condition and fully constrained condition. During the fracture process, the wire and the film were reported to exhibit multiple slip resulting in the neck formation after a strain of 1.0. Concentrated shear deformation with the localization of slip in the necked region was reported to result in ductile fracture. However, with the bulk specimen, they reported

the absence of necking by slip even at a strain of 1.0. The transformation was reported to be induced by the tensile strain. In the case of tension experiments with free transverse stress condition, i.e. without the constraint of transverse deformation, yielding was reported to be brought about by the crystallographic slip on the (1 1 1) planes at a strain of ~0:1. The yield stress in tension was found to be 15–20 GPa and very little difference in strength was reported between the wire, the film, and the bulk. Multiple slip even after yielding of the crystal and significant plastic deformation were reported to cause the ductile shear fracture. In the simulations with constraint of transverse deformation, the yield stress was reported to reach 40 GPa. No plastic strain was generated. This is attributed to the restriction of dislocation glide. Cleavage cracks were observed and found to bring about brittle fracture and hence a change in the fracture mode.

In this investigation, molecular dynamic simulation was carried out to study the effect on the mechanical properties of cobalt thin film under uniaxial and biaxial stress. The effect on the mechanical properties due to the change in cross section was also studied.

2. METHODOLOGY

Three-dimensional cobalt nanocrystalline sheets with various thicknesses between 2 and 10 nm were created by a computer code using LAMMPS with periodic boundary conditions in the three primary axes. The other two dimensions of nanosheets were kept 20 nm. The number of atoms in each sample varied from 74,000 to 362,640 according to film thickness. To perform molecular dynamics simulations using the LAMMPS code [13], EAM (embedded-atom method) potential was employed suggested by G. P. Purja Punand and Y. Mishin [14].

In the EAM formalism, the total energy of a collection of atoms is represented by,

$$E = \frac{1}{2}\sum_{i,j}\phi(r) + \sum_i F(\bar{\rho_i}), \qquad (1)$$

where $\phi(r_{ij})$ is a pair-interaction potential as a function of distance r between atoms i and $jF(\bar{\rho}_i)$ is the embedding energy as a function of the host electron density $\bar{\rho}_i$ on atom i. The electron density is the sum of atomic electron densities created at i by all other atoms of the system.

$$\overline{\rho} = \sum_{k\neq i}\rho(r_{i\,k}), \qquad (2)$$

The pair interactions are described by the generalized Lennard-Jones-type function.

$$\varphi(r) = \psi\left(\frac{r-r_c}{h}\right)\left[\frac{V_o}{b_2-b_1}\left(\frac{b_2}{(r/r_1)^{b_1}} - \frac{b_1}{(r/r_1)^{b_2}}\right) + \delta, \qquad (3)\right.$$

Equilibration simulations at NVE ensemble were performed for 50ps. NVE simulations were followed by a pressure equilibration for 150ps using NPT ensemble at atmospheric pressure. NVT simulations were done at 300K temperature for 10ps. An MD time step of 0.001ps was used for all the simulations considered in this study. The loading rate and temperature were kept constant at $10^9 s^{-1}$ and 300K respectively. The OVITO code [15] was employed to visualize and analyze the simulation results. Structural characterization of the simulated systems was performed using adaptive common neighbor analysis [16]. In order to visualize the structure of the simulated systems, atoms were colored according to their local structure order. The atoms with perfect HCP structure are shown as red, while those with perfect FCC structure are shown as green.

Fig. 1: An initial configuration of Co thin film with size of 20×20×10 nm.

3. RESULT AND DISCUSSION

3.1 Uniaxial Loading

The generated results of the molecular dynamics simulations are presented. The primary purpose of this work is to establish a relationship between film thickness and tensile strength. To elucidate that relationship, the stress vs. strain graph is presented in Fig 1.The figure shows two different types of responses. The stress either produce double peak meaning strain hardening or increasing, oscillating and then decreases. The stress increases linearly with strain up to a strain of 10%.

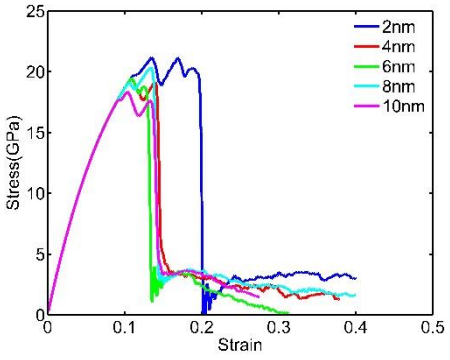

Fig. 2: Stress strain diagram at different thickness for uniaxial loading at 300Kand at strain rate of $10^9(s^{-1})$ legend shows thickness in nm

It can be seen that there is little variation in tensile strength between 4nm and 8nm while an overall decrease in strength is noticed. After the first peak, plastic deformation starts. Plastic deformation occurs due to propagation of the dislocation. From 10% to 20% strain it shows the flow of material. Variation of thickness has little effect on Young's modulus.

3.2 Biaxial Loading

From Fig. 3(a) and Fig. 3(b) shows similar mechanical properties along x-direction and y-direction. Figure 3(a) shows that there is no double peak in biaxial stress. Stress and strain had linear relation until 5% strain for all thicknesses. As thickness increased, tensile strength decreased. Fracture strain also showed an inverse relation with thickness. Thickness between 4nm to 8nm showed no variation in tensile strength and fracture strain but it was less than that of 2nm but more than that of 10nm.Variation of thickness has no effect on Young's modulus for biaxial tensile loading. From Fig. 4(a) it can be seen that fracture strain under uniaxial tensile loading is more than that of biaxial. Fig. 4(b) shows that modulus of elasticity under biaxial stress more than uniaxial. Fig. 4(c) shows that ultimate tensile strength under biaxial is more than that of uniaxial for each thickness. The only thickness not following this trend is 10nm which shows higher strength for 10nm.

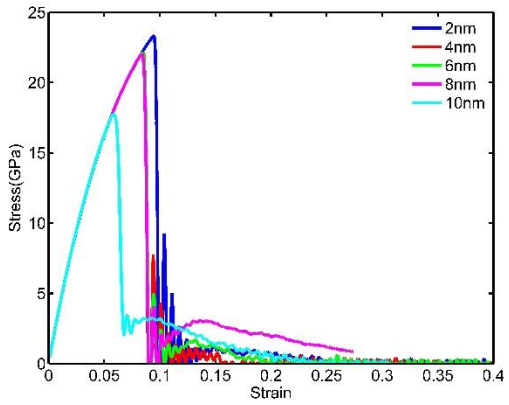

(a)

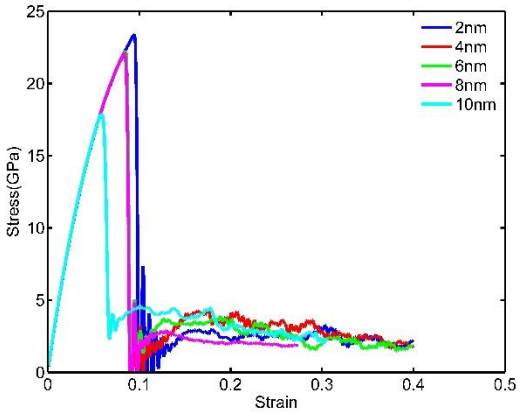

(b)

Fig. 3: Stress strain plot for different temperatures and biaxial loadings at (a) y direction (b) x direction at 300K and at the strain rate of $10^9 s^{-1}$ legend shows thickness in nm.

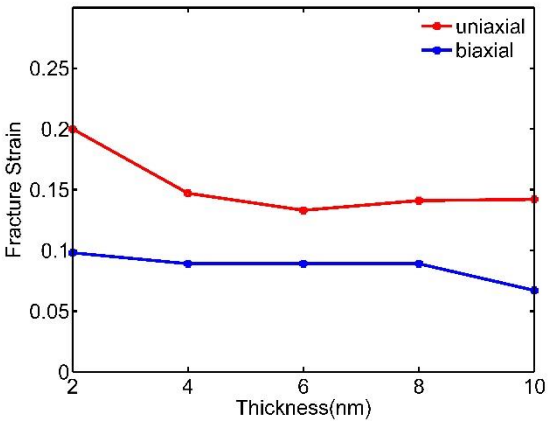

(a)

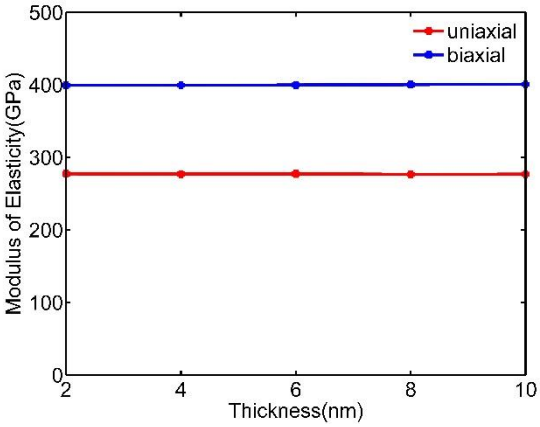

(b)

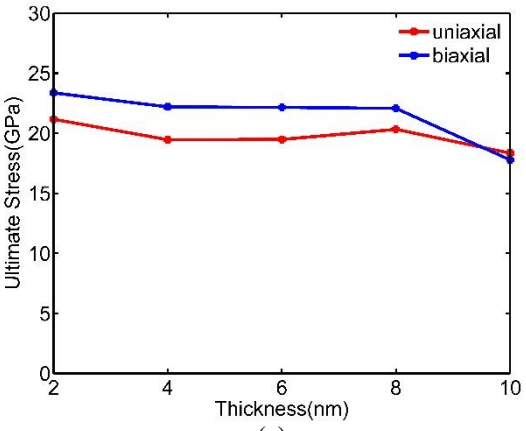

(c)

Fig. 4: Variation of (a) fracture strain, (b) Modulus of elasticity and (c) Ultimate stress with thickness at 300K and at a strain rate of $10^9 s^{-1}$.

3.3 Mechanism of Fracture

As we have simulated thin films having perfect crystal structures there is no effect of grain boundary based deformation mechanisms and crystal defects. Significant difference is observed between biaxial and uniaxial loading. In uniaxial loading, almost all films show double peak ductile type failure. Double peak indicates strain hardening [17]. HCP to FCC transformation is also observed during loading. Before failure percentage of FCC atoms for 2nm,4nm,6nm,8nm,10nm films are 78%,4.2%,4%,18.9% and 25.3% respectively.

In Fig. 4(a) the failure mechanism for thin film of thickness 2nm is shown. The fracture pattern is observed to follow typical behavior for perfect crystal. Fracture initiates via formation of small fissure in the structure due to the stress concentration at the strain value of 1.95 %. Fig. 4(a) and Fig. 4(b) shows the flow of materials at strain value of 10% to 20% for 2nm thickness. 2nm film is slightly different from other films and hence studied extensively. Stress concentration and movement of atoms with displacement vectors are shown for different values of strains.

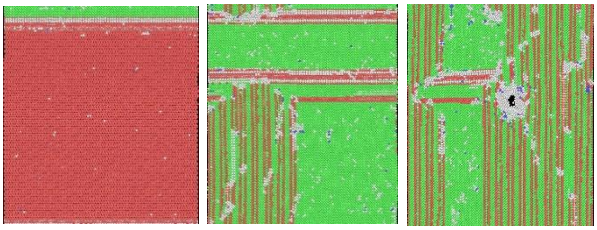

12% strain 19% strain 19.7% strain

(a)

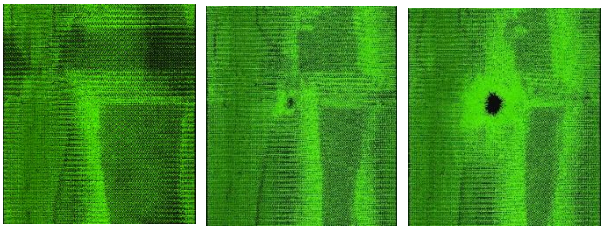

19.25% strain 19.66% strain 19.80% strain

(b)

Fig. 4: (a) Atomistic configurations of thin film of 2nm thickness at 300K at different stages (12%, 19%, 19.7% strain) of uniaxial tensile stress. Atoms are colored according to coordination number. Red represents HCP and green color FCC cobalt atoms (b) Displacement vectors of same thin film atoms at 300K at different stages (19.25% 19.66% 19.8%) for uniaxial tensile stress. Displacement vectors are shown in green color.

In Fig. 5 images of crystal when failure occurs is shown. Though crack initiation spot is different in different cases but considering periodic boundary condition we can say propagation is same for all films of different thicknesses in uniaxial loading.

Variation of values of ultimate stress and fracture strain is seen in uniaxial loading with film size. Thin films of 2nm and 10nm show the maximum and minimum values of ultimate stress and fracture strain respectively. Actually, for small sized nanosheets dislocations are generated and propagated within small dimensions but the large size nanosheets have enough space for dislocation propagation.

4nm to 10nm thin films shows a double peak in the plastic region and before fracture they show deformation twinning. HCP structure most likely to form deformation twin when they are strained [18]. In 4 nm wire (shown in Fig. 6), generated twins are responsible for crack initiation. The movement of dislocation is towards twin boundary which causes propagation of the crack. Multiple twin structure is formed at about 11.5%.

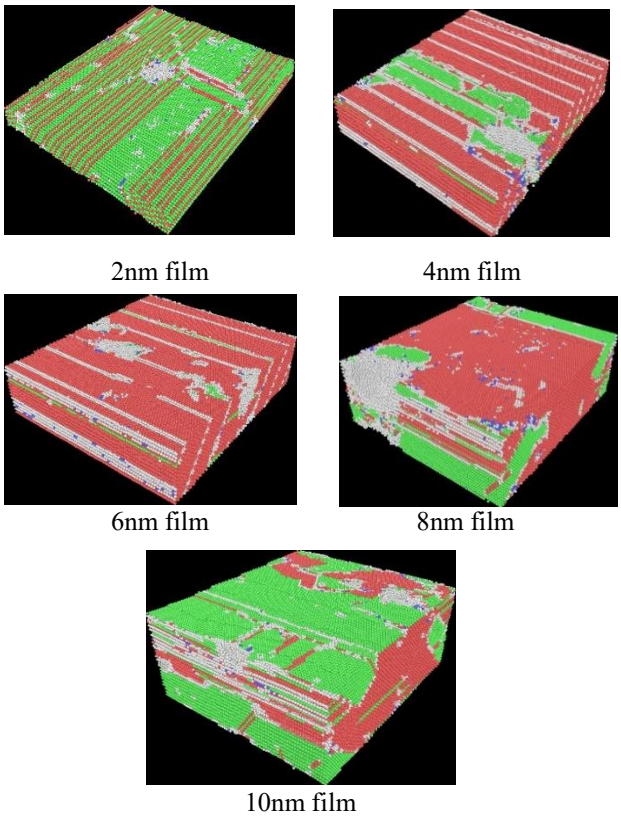

2nm film 4nm film

6nm film 8nm film

10nm film

Fig. 5: Atomistic configurations of fractured thin films of different thicknesses (2nm, 4nm, 6nm, 8nm, 10nm) at 300K of uniaxial tensile stress. Atoms are colored according to coordination number. Red represents HCP and green color FCC cobalt atoms.

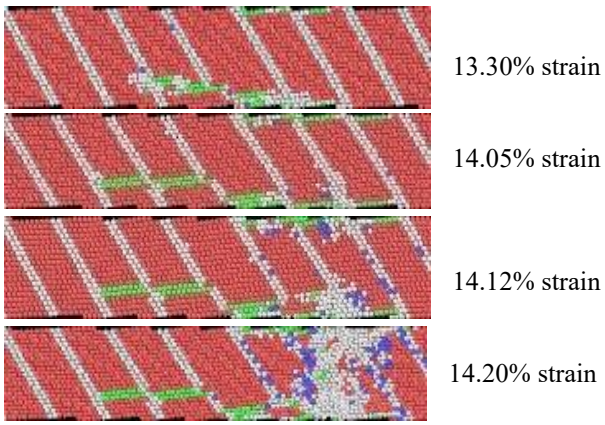

13.30% strain

14.05% strain

14.12% strain

14.20% strain

Fig. 6: Atomistic configurations of thin film of 4nm thickness at 300K at different stages (13.30%, 14.05%, 14.12%, 14.20% strain) of uniaxial tensile stress atoms are colored according to coordination number red represents HCP and green color FCC cobalt atoms.

In the case of biaxial loading, the failure criteria is totally different. Stress vs. strain plot Fig.3 for biaxial loading indicates brittle type behavior. Plots for all thicknesses shows single peak and sudden drop in value of stress. HCP to FCC transformation is not seen in biaxial loading. The percentage of FCC atoms before

loading is near to zero.

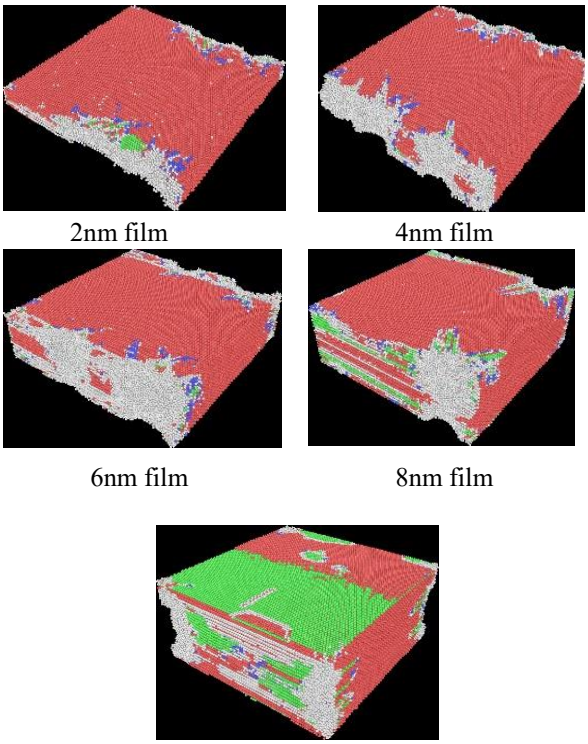

Fig. 7: atomistic configurations of fractured thinfilms of different thicknesses (2nm, 4nm, 6nm, 8nm, 10nm) at 300K of biaxial tensile stress. Atoms are colored according to coordination number. Red represents HCP and green color FCC cobalt atoms.

4. CONCLUSION

An MD simulation was employed to investigate the mechanical behavior of cobalt thin film the mechanical behavior of cobalt thin film using embed-atom model. The effect of thickness, uniaxial and biaxial loading were successfully studied. It was seen that fracture strength decreased as thickness increased while from 4 to 8nm showed no variation. The present model demonstrated that thickness has no significant effect on Young's modulus. The fracture strain seems to follow an inverse relation to thickness while thickness between 4nm and 6nm showed no variation. Finally for biaxial loading higher Young's modulus and ultimate strength was obtained.

5. ACKNOWLEDGEMENT

Authors of this article would like to thank Multiscale Mechanical Modeling and Research Networks (MMMRN) for their mentoring and guidance.

6. REFERENCES

[1] R.Komanduri, N.Chandrasekaran, and L.MRaff, "Molecular dynamic simulations of uniaxial tension at nanoscale of semiconductor materials for micro-electro-mechanical systems (MEMS) applications", *Materials Science and Engineering: A*, vol. 340, no. 1–2, pp. 58–67.

[2] R.Komanduri, N.Chandrasekarana, and L.M.Raff, "Molecular dynamics (MD) simulation of uniaxial tension of some single-crystal cubic metals at nanolevel", *International Journal of Mechanical Sciences*, vol. 43, no. 10, pp. 2237–2260, 2001.

[3] Harold S.Park, KenGall, and JonathanA.Zimmerman, "Deformation of FCC nanowires by twinning and slip", *Journal of the Mechanics and Physics of Solids*, vol. 54, no. 9, pp. 1862–1881, 2006.

[4] Harold S. Park and Jonathan A. Zimmerman, "Modeling inelasticity and failure in gold nanowires", *Phys. Rev. B*, vol. 72, no. 5, pp. 154–161, 2005.

[5] H.A.Wu, "Molecular dynamics study of the mechanics of metal nanowires at finite temperature", *European Journal of Mechanics – A/Solids*, vol. 25, no. 2, pp. 370–377, Apr. 2006.

[6] H.A.Wu, "Molecular dynamics study on mechanics of metal nanowire", *Mechanics Research Communications*, vol. 33, no. 1, pp. 9–16, 2006.

[7] I.F.Golovnev, E.I.Golovneva, and V.M.Fomin, "Molecular-dynamic modeling of mechanical properties of free defect metal nanocrystals", *Computational Materials Science*, vol. 37, no. 3, pp. 336–348, 2006.

[8] LinYuan, DebinShan, and BinGuo, "Molecular dynamics simulation of tensile deformation of nano-single crystal aluminum", *Journal of Materials Processing Technology*, vol. 184, no. 1–3, pp. 1–5, 2007.

[9] Paulo S. Branício and José-Pedro Rino, "Large deformation and amorphization of Ni nanowires under uniaxial strain: A molecular dynamics study", *PHYSICAL REVIEW B*, vol. 62, no. 24, pp. 169–180, 2000.

[10] Yu-HuaWen, Z.Z. Zhu, G.F. Shao, and R.Z. Zhu, "The uniaxial tensile deformation of Ni nanowire: atomic-scale computer simulations", *Physica E: Low-dimensional Systems and Nanostructures*, vol. 27, no. 1–2, pp. 113–120, 2005.

[11] M. Parrinello and A. Rahman, "Polymorphic transitions in single crystals: A new molecular dynamics method", *Journal of Applied Physics*, vol. 52, no. 12, pp. 7182–90, 1981.

[12] Kitamura T, Yashiro K, and Ohtani R, "Atomic Simulation on Deformation and Fracture of Nano-Single Crystal of Nickel in Tension", *JSME International Journal Series A Solid Mechanics and Material Engineering*, vol. 40, no. 4, pp. 430–435, 1997.

[13] Steve Plimpton, "Fast Parallel Algorithms for Short-Range Molecular Dynamics", *Journal of Computational Physics*, vol. 117, no. 1, pp. 1–19, 1995.

[14] G. P. Purja Pun and Y. Mishin, "Embedded-atom potential for hcp and fcc cobalt", *PHYSICAL REVIEW B*, vol. 86, no. 13, p. 134116, 2012.

[15] A.Stukowski, "Visualization and analysis of atomistic simulation data with OVITO–the Open Visualization Tool", *Modelling and Simulation in Materials Science and Engineering*, vol. 18, no. 1,

p.015012, 2010.
[16] A.Stukowski, “Structure identification methods for atomistic simulations of crystalline materials”, *Modelling and Simulation in Materials Science and Engineering*, vol. 20, no. 4, p. 045021.
[17] S.Saha, M.A.Motalab, and M.Mahboob, “Investigation on mechanical properties of polycrystalline W nanowire”, *Computational Materials Science*, vol. 136, pp. 52–59, 2017.
[18] Steinmetz, D.R, Jäpel, T., Wietbrock, B., Eisenlohr,P., Gutierrez-Urrutia,I, and Saeed, “Revealing the strain-hardening behavior of twinning-induced plasticity steels: Theory, simulations, experiments”, *Acta Materialia*, vol. 61, no. 2, pp. 494–510,2013.

7. NOMANCLETURE

Symbol	Meaning	Unit
E	Total Energy	eV
Q	Pair interaction potential	eV
r	distance	nm
r_c	Cutoff distance	nm
V	fitting parameter	eV
δ	fitting parameter	eV
F	embedding energy function	eV